Regular Article

Fabrication of Muco-Adhesive Oral Films by the 3D Printing of Hydroxypropyl Methylcellulose-Based Catechin-Loaded Formulations

Tatsuaki Tagami, Natsumi Yoshimura, Eiichi Goto, Takehiro Noda, and Tetsuya Ozeki*

Drug Delivery and Nano Pharmaceutics, Graduate School of Pharmaceutical Sciences, Nagoya City University; 3–1 Tanabe-dori, Mizuho-ku, Nagoya 467–8603, Japan.
Received June 10, 2019; accepted August 12, 2019

Pharmaceutical applications of three dimensional (3D) printing technology are increasing following the approval of 3D-printed tablets by the U.S. Food and Drug Administration. Semi-solid extrusion-type 3D printers are used to 3D print hydrogel- and paste-based materials. We previously developed tablet formulations for semi-solid extrusion-type 3D bioprinters. In the present study, we extended our study to the preparation of muco-adhesive oral film formulations to 3D bioprint mouth ulcer pharmaceuticals. We focused on hydroxypropyl methylcellulose (HPMC)-based catechin (model drug)-loaded hydrogel formulations and found that the viscosity of a hydrogel formulation is dependent on the HPMC concentration, and that viscosity is important for facile 3D printing. HPMC-based films were prepared using two different drying methods (air drying and freeze drying). The films exhibited different drug dissolution profiles, and increasing the amount of HPMC in the film delayed drug dissolution. The fabrication of HPMC-based catechin-loaded films with different shapes provides a model of individualized, on-demand pharmaceuticals. Our results support the flexible application of 3D bioprinters (semi-solid extrusion-type 3D printers) for preparing film formulations.

Key words three dimensional (3D) printing; mucoadhesive oral film; personalized therapy; pressure-assisted microsyringe (PAM) printing; semi-solid extrusion

INTRODUCTION

Three-dimensional (3D) printing technologies are currently finding applications in medicine.[1,2] Rapid prototyping is a common use of 3D printing to develop approaches for efficiently designing and manufacturing parts such as jigs and entire devices. Various medical devices[3,4] and imaging phantoms[5] have been produced using 3D printers. 3D printing of a surgical site is useful for understanding the pathology of the site before surgery and for aiding patient understanding of their condition prior to giving consent for surgery. The internet site ClinicalTrial.gov (URL: https://clinicaltrials.gov/) has registered many clinical trials related to "3D printing." Most clinical trials involving 3D printing of surgical guides and anatomical models currently aim to facilitate the planning of musculoskeletal surgery and oral/maxillofacial surgery,[6] although several recent clinical trials have involved the 3D printing of implants for addressing bone defects and breast reconstruction for individual patients. 3D printing of cells (bioprinting) also holds promise for patient-specific tissue fabrication as a regeneration therapy.[7,8] The contribution of 3D printing technology to personalized medical therapy is thus clearly expanding.

New pharmaceutical applications of 3D printing technology are increasing following the U.S. Food and Drug Administration approval of the manufacturing of a 3D printed tablet (SPRITAM) in August 2015.[9,10] This orodispersible tablet is manufactured in bulk using a powder-based 3D printer and ZipDose technology. Other types of 3D printers using various printer materials have been studied to explore novel applications of 3D printed pharmaceuticals. For example, Khaled *et al.* reported the preparation of a polypill (a multiple active pharmaceutical tablet) using a multi-nozzle-equipped semi-solid extrusion type 3D printer.[11,12] Additionally, tablets with unique designs and geometries prepared by 3D printing allow controlled drug release.[13–16] Polypills and novel tablets manufactured using a 3D printer may allow personalized dosing, an important advancement since each patient has unique pharmacokinetics and metabolism. The use of 3D printers for preparing pharmaceutical doses may change both drug manufacturing and therapeutic approaches.

We previously reported the preparation of tablets using a pressurized air semi-solid extrusion-type 3D bioprinter to extrude bio-ink.[17] 3D bioprinters have been studied for possible applications in tissue engineering, for example by using hydrogel/paste-based materials to prepare cell-incorporated bio-inks. The manufacture of skin and body parts using a 3D bioprinter holds promise for future transplantation therapy,[18] and 3D printing of organs-on-a-chip (*e.g.*, liver) that can replicate organ-level functions which would transform the screening and testing of drugs.[19,20] Pharmaceutical applications of 3D bioprinters may allow the preparation of temperature-sensitive drugs and biopharmaceuticals by using a hydrogel/paste-based drug formulation[17] because bioprinters do not require high temperature, in contrast to typical 3D printers (*e.g.*, the conventional fused deposition modeling (FDM)-type 3D printer used to prepare tablets).

The aim of this study was to extend the application of tailored 3D-printed pharmaceuticals to muco-adhesive oral films composed of hydroxypropyl methylcellulose (HPMC) using catechin as a model drug. This novel film formulation would treat inflammations of the oral cavity such as aphthous stomatitis and oral mucositis ulcers. Aphthous stomatitis is a common mucosal disorder caused by biting, acidic foods,

* To whom correspondence should be addressed. e-mail: ozekit@phar.nagoya-cu.ac.jp

© 2019 The Pharmaceutical Society of Japan

smoking, and various immune reactions due to systemic and viral diseases.[21] Oral mucositis ulcers occur in cancer patients following radiation therapy and chemotherapy.[22,23] Catechins are flavonoids and polyphenols found in tea leaf and exhibit anti-oxidant, anti-inflammatory, anti-cancer, and anti-hypertensive effects.[24] The use of catechin-based films may help alleviate oral ulcers when combined with standard treatments.

Muco-adhesive buccal films and orodispersible films are attracting considerable interest as new oral formulations for local and systemic drug administration.[25] The properties of HPMC-based muco-adhesive films prepared by traditional casting methods have been reported,[26,27] and the preparation of oral films with different doses and shapes is important for personalized dosing and therapy. Film formulations have been prepared using inkjet-type and flexographic-type 2D printers[28–30] and a FDM-type 3D printer,[25,31–33] whereas to our knowledge there have been no reports describing the preparation of drug-loaded oral muco-adhesive film formulations using a 3D bioprinter. Here we characterized printer-inks (HPMC-based hydrogels containing a drug) and the resulting films (dried 3D-printed films).

MATERIALS AND METHODS

Reagents HPMC (METOLOSE 90SH-15000SR HPMC 2208 type) was supplied by Shin-Etsu Chemical Company, Ltd. (Tokyo, Japan). D(−)-Mannitol, Tween 20, Tween 80, glycerol and ethanol were purchased from Wako Pure Chemical Industries, Ltd. (Osaka, Japan). (+)-Catechin hydrate was purchased from Sigma-Aldrich (St. Louis, MO, U.S.A.).

Preparation of Hydrogel-Based Printer Inks HPMC hydrogel-based drug formulations were prepared as printer inks as previously reported, with modification.[34] Water (7 mL) and a magnetic stirrer were added in a screw-top glass vial and placed in a water bath at 80°C, then appropriate amounts of HPMC powder and mannitol were added to the vial with stirring. Catechin (50 mg) was dissolved in 3 mL ethanol/water (2/1, v/v), heated to 80°C and added to the vial, followed by 40 μL each Tween 80 and glycerol at 80°C and the solution was stirred well. The drug formulations are described in Table 1. The vial was cooled and kept at room temperature overnight to remove bubbles.

Viscosity Characteristics of the Printer Ink The viscosity of each sample was measured using a rotational cone-plate viscometer (Brookfield viscometer DV2T, Brookfield, Middleboro, MA, U.S.A.) with a CPE-40 or CPE-52 spindle (Brookfield) at 25°C. The rotation speed was gradually increased (0.1, 0.2, 0.5, 1, 2, 5, 10, 20, 50, 100 and 200 rpm) every 30 s, and the shear stress and viscosity were measured.

3D Design and Printing, and Preparation of the Films Film-like sheets ($40 \times 40 \times 0.35$ mm) was designed using 123D Design 3D CAD software (Autodesk Inc., San Rafael, CA, U.S.A.) (Fig. 1A). The 3D printing conditions were set using Slic3r slicer software (GNU General Public License) (Fig. 1B). The printer ink prepared as described in previous section was carefully loaded into a syringe with a 27G nozzle, then set in the 3D bioprinter (INKREDIBLE; CELLINK; Gothenburg, Sweden). A clear polypropylene sheet was placed on the 3D printer stage to support film-like hydrogel sheets printed by the extrusion of printer ink from the nozzle (Fig. 1C). The extrusion of ink was controlled by using the air pressure through pump (Formulation B, 20 kPa; Formulation C, 50 kPa; Formulation D, 70 kPa, as a typical experiment). The printed hydrogel was air dried at room temperature (air drying method, AD method) and stored in a desiccator. Alternatively, the hydrogel was frozen at −80°C and freeze-dried using a FD1000 freeze-dryer (EYELA, Tokyo, Japan) (freeze drying method, FD method).

Measurement of Film Weights and Thicknesses The weights of film samples after drying were measured on an electric balance. The thicknesses of film samples were measured at five randomly selected points using a digital micrometer to the nearest 0.001 mm (MDC-25MX, Mitutoyo, Kawasaki, Japan).

Dissolution Test Dissolution tests of the film formulations were conducted using paddle-type methods according to Japanese Pharmacopoeia 17th edition and a reference.[35] The dissolution vessel was placed in the dissolution tester (NTR-6200 A; Toyama Sangyo, Osaka, Japan) and 300 mL 0.1% Tween 20 was added. The temperature of the solution was maintained at 37°C and the stir rate was 50 rpm. Films prepared in previous section were folded, individually inserted into a metal sinker to prevent the sample from floating, then placed in the vessel. Aliquots of sample solution were col-

Table 1. Compositions of the HPMC-Based 3D Printer Inks Used in This Study

(A)

Formulation	HPMC (mg)	Catechin (mg)	Mannitol (mg)	Water (mL)	Ethanol (mL)	Tween (mL)	Glycerol (mL)
A	100	0	200	8.0	2.0	0.040	0.040
B	200	0	200	8.0	2.0	0.040	0.040
C	300	0	200	8.0	2.0	0.040	0.040
D	400	0	200	8.0	2.0	0.040	0.040
E	500	0	200	8.0	2.0	0.040	0.040

(B)

Formulation	HPMC (mg)	Catechin (mg)	Mannitol (mg)	Water (mL)	Ethanol (mL)	Tween (mL)	Glycerol (mL)
A′	100	50	150	8.0	2.0	0.040	0.040
B′	200	50	150	8.0	2.0	0.040	0.040
C′	300	50	150	8.0	2.0	0.040	0.040
D′	400	50	150	8.0	2.0	0.040	0.040
E′	500	50	150	8.0	2.0	0.040	0.040

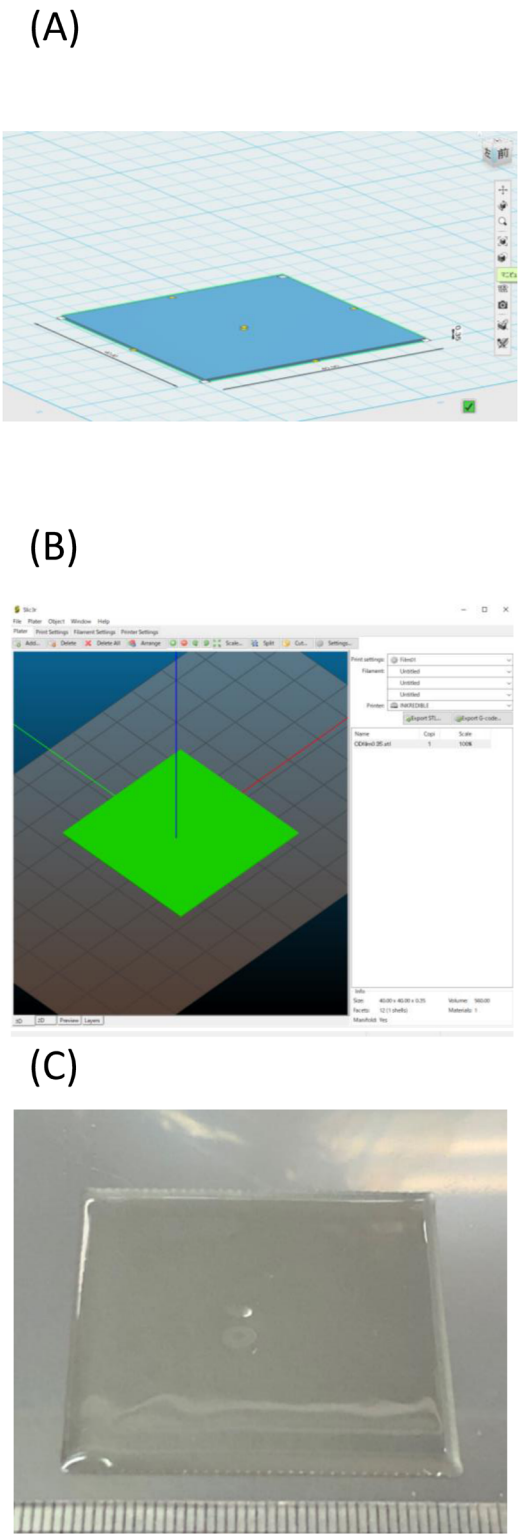

Fig. 1. Scheme Showing Film Preparation

(A) 3D design of a film sheet using 3D CAD software. (B) 3D printing program settings. (C) 3D printed film sheet. (Color figure can be accessed in the online version.)

lected at appropriate time points and the same volume of 0.1% Tween 20 solution was injected. The concentration of drug in solution was determined by measuring the absorbance of each aliquot at 280 nm using an UV visible spectrometer (UV1800; Shimadzu, Kyoto, Japan).

Scanning Electron Microscopy (SEM) The film samples were observed by SEM (S-4300, Hitachi; Tokyo, Japan) after coating with Pt–Pd using an ion sputtering apparatus (E-102; Hitachi).

Powder X-Ray Diffraction Film and powder samples were analyzed by powder X-ray diffraction measurements using a Rint-Ultima (Rigaku Co., Ltd., Tokyo, Japan) by irradiating with Cu-$K\alpha$ X-rays. The tube voltage and amperage were 44 kV and 40 mA, respectively. Samples were scanned between 2θ of 3 to 45°.

RESULTS AND DISCUSSION

Viscosity Characteristics of the HPMC Hydrogel-Based Printer Inks We first prepared drug-loaded hydrogel formulations as 3D bioprinter inks. The film formulations consist of an active pharmaceutical ingredient, water soluble polymer, sweetening agent, surfactant, plasticizer, and other components (*e.g.*, saliva stimulating agent, flavors, colors, fillers).[36] The drug formulations are described in Table 1. HPMC, mannitol, Tween, and glycerol were used as the water-soluble polymer, sweetening agent, surfactant, and plasticizer, respectively.

The viscosities of drug formulations with different concentrations of HPMC (Formulation A′–E′) were measured because the polymer concentration greatly affects viscosity, which in turn affects extrusion of the printer-ink from the nozzle. Printer-ink with a low viscosity can leak from the nozzle while ink with a high viscosity is difficult to handle and extrude. Consequently, the viscosity of the ink must be regulated to prepare pharmaceutical-quality film formulations using an extrusion-type 3D bioprinter.

The rheological properties of the drug-loaded printer-inks are shown in Fig. 2. The rheogram (relationship between shear stress and shear rate) changed as the concentration of HPMC changed (1–5%, Formulation A′–E′). The formulation with the lowest HPMC concentration (Formulation A′) provided an almost linear relationship (Fig. 2A), indicating Newtonian flow, as well as the lowest viscosity of the five formulations (Fig. 2F) which resulted in its leakage from the bioprinter nozzle. In contrast, the formulation with the highest HPMC concentration (Formulation E′, Figs. 2E, F) was difficult to extrude from the nozzle. Formulation B′–D′ appeared suitable for 3D printing through the 27G nozzle. The particle size of hydrophobic drugs and excipients in formulations must be controlled to prevent nozzle clogging. The HPMC-based hydrogel formulations prepared in the present study are clear and dissolved and thus suitable as printer-inks for extrusion-type 3D printers.

The rheograms of these formulations are shown in Figs. 2C and D and indicate that the formulations are stable against stress which are lower than yield value (stress). Higher stress can result in material flow. The application of strong air pressure can cause the printer ink to extrude and the printed hydrogel retains its shape without collapsing under its weight. We believe that the viscosity properties of our formulations are useful for 3D printing, as supported by our previous 3D bioprinting of tablets.[17] The viscosity characteristics of formulations without drug (Formulation A–E) are shown in Supplementary Fig. 1 and are very similar to the corresponding drug-containing formulation (Formulation A′–E′), showing that the viscosity of the printer ink was dependent on the con-

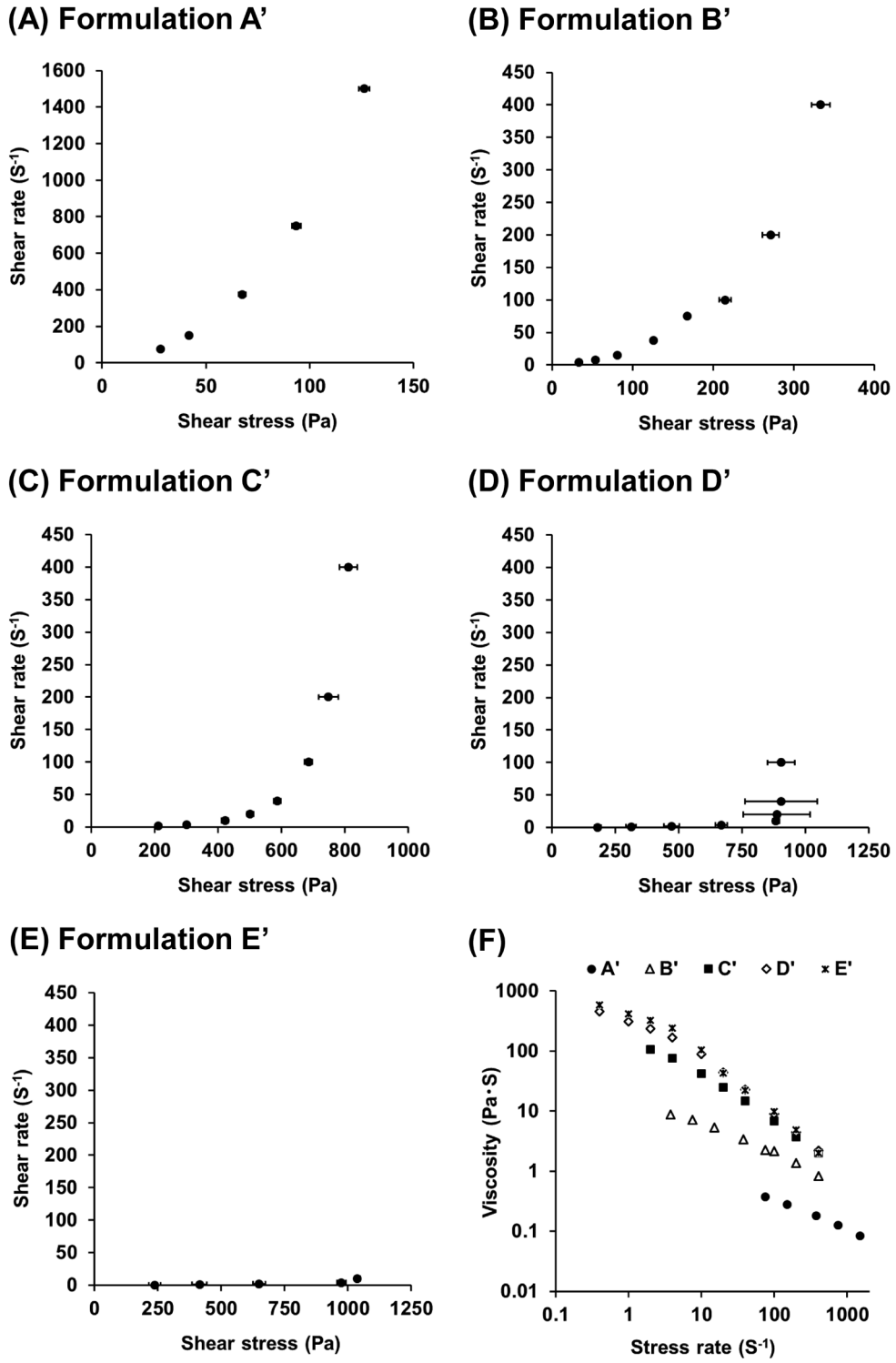

Fig. 2. Shear Stress–Shear Rate Data for HPMC-Based Drug-Loaded Formulations

(A–E) Formulation A′–E.′ (F) Viscosity–shear rate data. The data show the means ± standard deviation (S.D.) ($n = 3$).

centration of HPMC.

Film Preparation by Drying 3D Printed Hydrogel Formulations and Film Characteristics Film-like hydrogel sheets were 3D printed (Fig. 1C) and the HPMC-based films were obtained by drying, as shown in Fig. 3. Two types of films were prepared using two drying methods. The first was the simple AD method (Figs. 3A, C, E). Increasing the amount of HPMC resulted in the formation of suitable clear films (Fig. 3E) whereas films with insufficient HPMC were white, indicating crystallization of the mannitol and drug. Films formed using formulation B′-AD were very scratch-resistant (Fig. 3A). In the present study, 50 mg catechin was incorporated in the hydrogel stock formulation (Table 1B). The increase of catechin may have the possibility to crystallize the drug and to affect the appearance of air-dried film. We also prepared films using the FD method (Figs. 3B, D, F) and obtained cotton-like fine films using all three formulations. The weights and thicknesses of films prepared by the two methods are shown

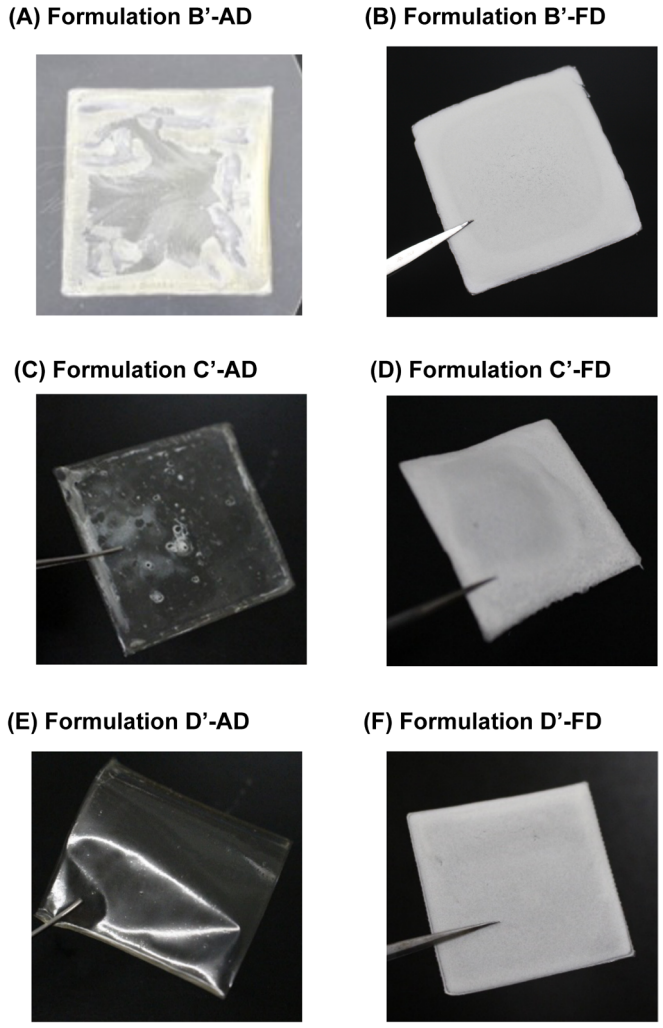

Fig. 3. Appearance of AD Films and FD Films
(Color figure can be accessed in the online version.)

Table 2. Characteristics of Catechin-Loaded 3D Printed Oral Films Dried Using Two Different Methods

(A)			
Formulation	Weight (mg)	Drug (mg)	Thickness (μm)
B′-AD	50.9 ± 9.0	5.2 ± 0.9	N.D.
C′-AD	40.5 ± 3.3	3.4 ± 0.3	38 ± 6
D′-AD	46.7 ± 7.1	3.4 ± 0.5	33 ± 3
(B)			
Formulation	Weight (mg)	Drug (mg)	Thickness (μm)
B′-FD	51.0 ± 11.6	5.2 ± 1.2	398 ± 49
C′-FD	33.9 ± 3.5	2.9 ± 0.3	358 ± 73
D′-FD	45.7 ± 7.5	3.3 ± 0.6	352 ± 43

The data show the means ± S.D. ($n = 5$).

in Table 2. The weights of the films were similar using both methods but the thicknesses varied greatly, with FD samples being almost 10-times thicker than AD samples due to differences in the preparation method.

The *in vitro* dissolution profiles of drugs from the films are shown in Fig. 4. The B′-AD film was difficult to scratch,

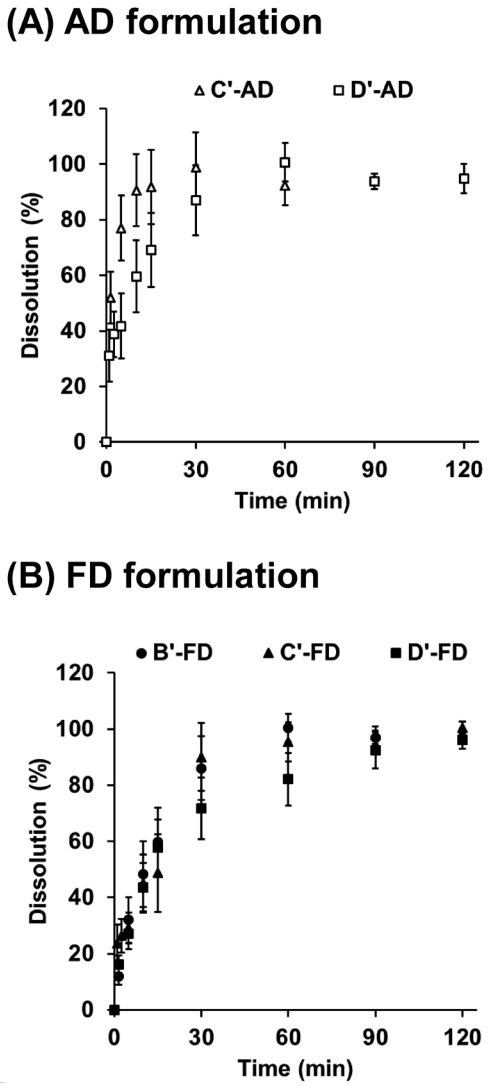

Fig. 4. Drug Dissolution Profiles from (A) AD Films and (B) FD Films
The data show the means ± S.D. ($n = 3$).

and thus, we tested two AD formulations (Formulation C′-AD and D′-AD) and three FD formulations (Formulation B′-FD, C′-FD, D′-AD). Formulation D′-AD and D′-FD exhibited delayed drug dissolution, suggesting that gel formation around the surface of these HPMC-based films controlled drug release. The drug release profile of HPMC matrix drug tablets has been investigated in detail.[37] Increasing the amount of HPMC in a film delays dissolution, thereby controlling drug dissolution. Additionally, HPMC is adhesive and thus is used as a binder. Moistened HPMC-based film in the oral cavity is likely muco-adhesive and releases drug locally in a controlled manner, depending on the amount of HPMC.

Jamroz *et al.*, prepared aripiprazole-loaded orodispersible film by using FDM-type 3D printer.[33] The 3D printing which is additive manufacturing process can produce the pore (about $650 \times 300\,\mu$m) in the film structure, and the drug dissolution from film was increased compared with the film prepared by conventional casting method due to the increase of surface area. If we produced the film with the pore and lattice by using semi-solid extrusion type 3D printer, it could change the drug dissolution. The high degree of freedom in design is a potential advantage of 3D printing.

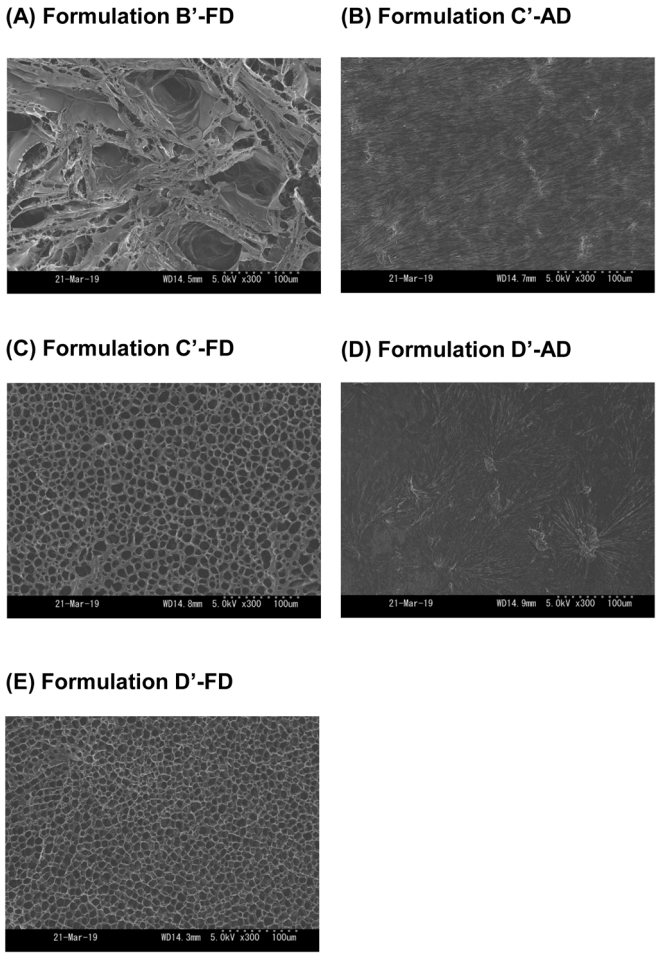

Fig. 5. Surface Appearance of AD Films and FD Films as Observed by SEM

We next studied the microstructures of the films by obtaining SEM images (Fig. 5). FD films have porous structures (Figs. 4A, C, E) and AD films do not. The amount of HPMC in the films may affect the porous structure. Films formed using Formulation B′-AD contain low amounts of HPMC and had rough and large pores whereas films formed using Formulations C′-FD and D′-FD contain higher amounts of HPMC and had small pores. These differences in microstructure did not greatly affect drug dissolution (Fig. 4), likely because the simple geometry (film) has a minimum effect on drug dissolution using the current experimental conditions. Drug dissolution from Formulation C′-AD was unexpectedly faster than that from formulation C′-FD (Fig. 4). We had assumed that FD films with porous structures would lead to rapid drug dissolution due to the large surface area, but the opposite results were obtained, perhaps because the different thickness between AD and FD samples affected drug release (FD samples were approximately 10-times thicker, as shown in Table 2). Physical properties were assessed using powder X-ray diffraction (Fig. 6). The strong mannitol and relatively weak catechin peaks in AD and FD formulations (Formulation D′-AD and D′-FD) disappeared due to amorphous state of HPMC.

Preparation of Films for Personalized Therapy Using a Semi-solid Extrusion-Type 3D Bioprinter As shown in Fig. 7, various designs and shapes of AD and FD films were designed and prepared. Aphthous stomatitis is typically characterized by small, round or ovoid ulcers[38] whereas the shapes of mouth ulcers formed by cheek bites differ depending on the strength of the bite. The shape of oral mucositis induced by

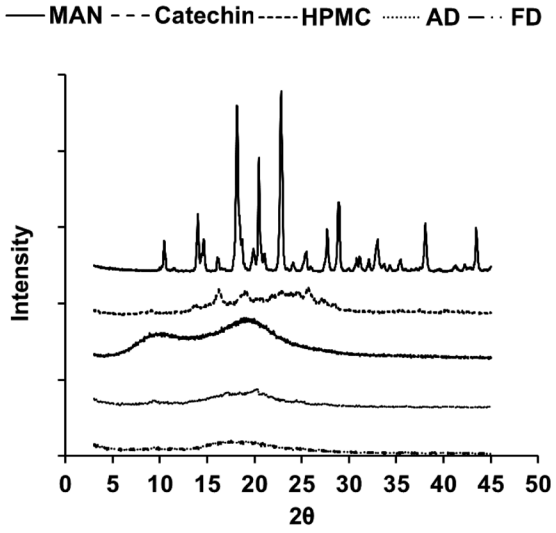

Fig. 6. Mannitol, Catechin, HPMC, AD Film and FD Film Powder X-Ray Diffraction Patterns

Formulations D′-AD and D′-FD, described in Table 2, were used as the film samples.

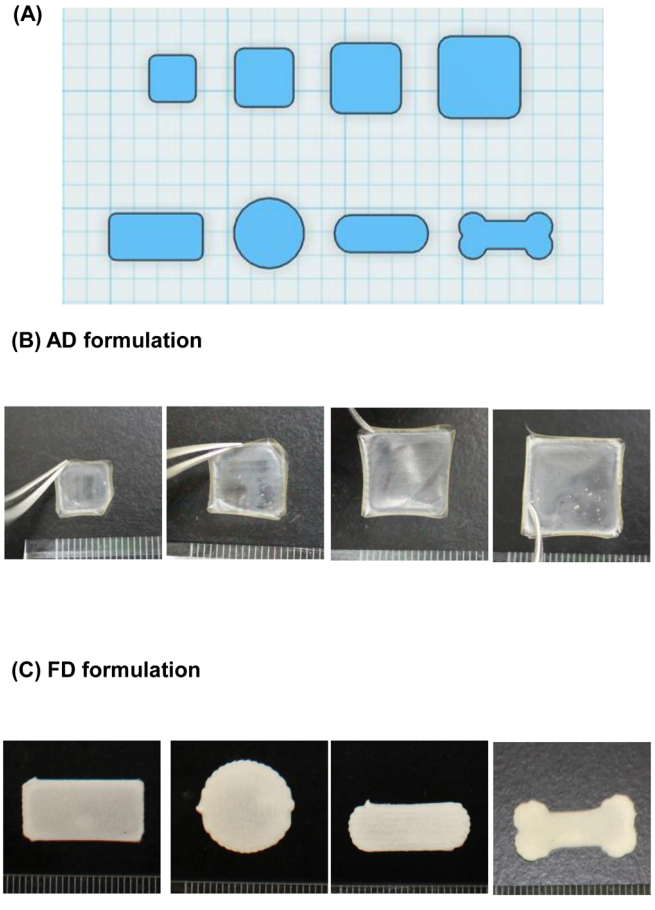

Fig. 7. Preparation of Personalized Oral Films Using a Semi-solid Extrusion-Type 3D Printer

(A) 3D designs of various film shapes, (B) AD films, and (C) FD films. Formulations D′-AD and D′-FD, described in Table 2, were used as the film samples. (Color figure can be accessed in the online version.)

radiation therapy and chemotherapy also vary depending on the individual and thus we attempted to prepare individualized films with desired shapes using a semi-solid extrusion-type 3D bioprinter as model 3D printed tailored pharmaceuticals. 3D printed manufacturing of personalized pharmaceuticals was previously proposed.[39] An electronic prescription is sent from a hospital department to a 3D printer, and raw materials in the printer ink are used to manufacture formulations (tablets) using a 3D printer under quality control *via* process analysis technology. Film formulations are likely also applicable to this concept, since 3D bioprinters can handle several types of drug formulations. The present study showed the probable utility of 3D bioprinters in clinical settings.

CONCLUSION

In conclusion, we focused on identifying appropriate printing conditions for drug formulations of HPMC-based hydrogels by varying the polymer concentration, and hence the viscosity, of prepared AD and FD films. FD films appear to be advantageous for preparing films because all FD films were easy to handle, of the appropriate thickness, and had good visual characteristics. The present study provides useful information on a model pharmaceutical for personalized therapy generated using a semi-solid extrusion-type 3D printer.

Acknowledgments This research was partly supported by a Grant-in-Aid for Scientific Research from the Japan Society for the Promotion of Science (19K07170).

Conflict of Interest The authors declare no conflict of interest.

Supplementary Materials The online version of this article contains supplementary materials.

REFERENCES

1) Liaw CY, Guvendiren M. Current and emerging applications of 3D printing in medicine. *Biofabrication*, **9**, 024102 (2017).
2) Garcia J, Yang Z, Mongrain R, Leask RL, Lachapelle K. 3D printing materials and their use in medical education: a review of current technology and trends for the future. *BMJ Simul. Technol. Enhanc. Learn.*, **4**, 27–40 (2018).
3) Aran K, Chooljian M, Paredes J, Rafi M, Lee K, Kim AY, An J, Yau JF, Chum H, Conboy I, Murthy N, Liepmann D. An oral microjet vaccination system elicits antibody production in rabbits. *Sci. Transl. Med.*, **9**, eaaf6413 (2017).
4) Nagai N, Koyanagi E, Izumida Y, Liu J, Katsuyama A, Kaji H, Nishizawa M, Osumi N, Kondo M, Terasaki H, Mashima Y, Nakazawa T, Abe T. Long-term protection of genetically ablated rabbit retinal degeneration by sustained transscleral unoprostone delivery. *Invest. Ophthalmol. Vis. Sci.*, **57**, 6527–6538 (2016).
5) Filippou V, Tsoumpas C. Recent advances on the development of phantoms using 3D printing for imaging with CT, MRI, PET, SPECT, and ultrasound. *Med. Phys.*, **45**, e740–e760 (2018).
6) Diment LE, Thompson MS, Bergmann JHM. Clinical efficacy and effectiveness of 3D printing: a systematic review. *BMJ Open*, **7**, e016891 (2017).
7) Patra S, Young V. A review of 3D printing techniques and the future in biofabrication of bioprinted tissue. *Cell Biochem. Biophys.*, **74**, 93–98 (2016).
8) Nagarajan N, Dupret-Bories A, Karabulut E, Zorlutuna P, Vrana NE. Enabling personalized implant and controllable biosystem development through 3D printing. *Biotechnol. Adv.*, **36**, 521–533 (2018).
9) Alam MS, Akhtar A, Ahsan I, Shafiq-Un-Nabi S. Pharmaceutical product development exploiting 3D printing technology: conventional to novel drug delivery system. *Curr. Pharm. Des.*, **24**, 5029–5038 (2018).
10) Jamroz W, Kurek M, Lyszczarz E, Brniak W, Jachowicz R. Printing techniques: recent developments in pharmaceutical technology. *Acta Pol. Pharm.*, **74**, 753–763 (2017).
11) Khaled SA, Burley JC, Alexander MR, Yang J, Roberts CJ. 3D printing of five-in-one dose combination polypill with defined immediate and sustained release profiles. *J. Control. Release*, **217**, 308–314 (2015).
12) Khaled SA, Burley JC, Alexander MR, Yang J, Roberts CJ. 3D printing of tablets containing multiple drugs with defined release profiles. *Int. J. Pharm.*, **494**, 643–650 (2015).
13) Korte C, Quodbach J. 3D-printed network structures as controlled-release drug delivery systems: dose adjustment, API release analysis and prediction. *AAPS PharmSciTech*, **19**, 3333–3342 (2018).
14) Martinez PR, Goyanes A, Basit AW, Gaisford S. Influence of geometry on the drug release profiles of stereolithographic (SLA) 3D-printed tablets. *AAPS PharmSciTech*, **19**, 3355–3361 (2018).
15) Arafat B, Wojsz M, Isreb A, Forbes RT, Isreb M, Ahmed W, Arafat T, Alhnan MA. Tablet fragmentation without a disintegrant: a novel design approach for accelerating disintegration and drug release from 3D printed cellulosic tablets. *Eur. J. Pharm. Sci.*, **118**, 191–199 (2018).
16) Tagami T, Nagata N, Hayashi N, Ogawa E, Fukushige K, Sakai N, Ozeki T. Defined drug release from 3D-printed composite tablets consisting of drug-loaded polyvinylalcohol and a water-soluble or water-insoluble polymer filler. *Int. J. Pharm.*, **543**, 361–367 (2018).
17) Tagami T, Ando M, Nagata N, Goto E, Yoshimura N, Takeuchi T, Noda T, Ozeki T. Fabrication of naftopidil-loaded tablets using a semisolid extrusion-type 3D printer and the characteristics of the printed hydrogel and resulting tablets. *J. Pharm. Sci.*, **108**, 907–913 (2019).
18) Cubo N, Garcia M, Del Canizo JF, Velasco D, Jorcano JL. 3D bioprinting of functional human skin: production and *in vivo* analysis. *Biofabrication*, **9**, 015006 (2016).
19) Lee H, Chae S, Kim JY, Han W, Kim J, Choi Y, Cho DW. Cell-printed 3D liver-on-a-chip possessing a liver microenvironment and biliary system. *Biofabrication*, **11**, 025001 (2019).
20) Yi HG, Lee H, Cho DW. 3D printing of organs-on-chips. *Bioengineering*, **4**, 10 (2017).
21) Scully C, Porter S. Oral mucosal disease: recurrent aphthous stomatitis. *Br. J. Oral Maxillofac. Surg.*, **46**, 198–206 (2008).
22) Russo G, Haddad R, Posner M, Machtay M. Radiation treatment breaks and ulcerative mucositis in head and neck cancer. *Oncologist*, **13**, 886–898 (2008).
23) Jensen SB, Peterson DE. Oral mucosal injury caused by cancer therapies: current management and new frontiers in research. *J. Oral Pathol. Med.*, **43**, 81–90 (2014).
24) Cabrera C, Artacho R, Giménez R. Beneficial effects of green tea—a review. *J. Am. Coll. Nutr.*, **25**, 79–99 (2006).
25) Speer I, Preis M, Breitkreutz J. Novel dissolution method for oral film preparations with modified release properties. *AAPS PharmSciTech*, **20**, 7 (2019).
26) Yehia SA, El-Gazayerly ON, Basalious EB. Fluconazole mucoadhesive buccal films: *in vitro*/*in vivo* performance. *Curr. Drug Deliv.*, **6**, 17–27 (2009).
27) Perioli L, Ambrogi V, Angelici F, Ricci M, Giovagnoli S, Capuccella M, Rossi C. Development of mucoadhesive patches for buccal administration of ibuprofen. *J. Control. Release*, **99**, 73–82 (2004).
28) Wickström H, Palo M, Rijckaert K, Kolakovic R, Nyman JO, Määttänen A, Ihalainen P, Peltonen J, Genina N, de Beer T, Löbmann K,

Rades T, Sandler N. Improvement of dissolution rate of indomethacin by inkjet printing. *Eur. J. Pharm. Sci.*, **75**, 91–100 (2015).
29) Raijada D, Genina N, Fors D, Wisaeus E, Peltonen J, Rantanen J, Sandler N. A step toward development of printable dosage forms for poorly soluble drugs. *J. Pharm. Sci.*, **102**, 3694–3704 (2013).
30) Janssen EM, Schliephacke R, Breitenbach A, Breitkreutz J. Drug-printing by flexographic printing technology—a new manufacturing process for orodispersible films. *Int. J. Pharm.*, **441**, 818–825 (2013).
31) Musazzi UM, Selmin F, Ortenzi MA, Mohammed GK, Franzé S, Minghetti P, Cilurzo F. Personalized orodispersible films by hot melt ram extrusion 3D printing. *Int. J. Pharm.*, **551**, 52–59 (2018).
32) Ehtezazi T, Algellay M, Islam Y, Roberts M, Dempster NM, Sarker SD. The application of 3D printing in the formulation of multilayered fast dissolving oral films. *J. Pharm. Sci.*, **107**, 1076–1085 (2018).
33) Jamróz W, Kurek M, Lyszczarz E, Szafraniec J, Knapik-Kowalczuk J, Syrek K, Paluch M, Jachowicz R. 3D printed orodispersible films with Aripiprazole. *Int. J. Pharm.*, **533**, 413–420 (2017).
34) Manasa B, Gudas GK, Sravanthi N, Madhuri RA, Lavanya Y, Pranitha C. Formulation and evaluation of mucoadhesive buccal patches of resperidone. *J. Chem. Pharm. Res.*, **2**, 866–872 (2010).
35) Takeuchi Y, Usui R, Ikezaki H, Tahara K, Takeuchi H. Characterization of orally disintegrating films: a feasibility study using an electronic taste sensor and a flow-through cell. *J. Drug Deliv. Sci. Tech.*, **39**, 104–112 (2017).
36) Kalyan S, Bansal M. Recent trends in the development of oral dissolving film. *Int. J. Pharm. Tech. Res.*, **4**, 725–733 (2012).
37) Siepmann J, Peppas NA. Modeling of drug release from delivery systems based on hydroxypropyl methylcellulose (HPMC). *Adv. Drug Deliv. Rev.*, **48**, 139–157 (2001).
38) Scully C. Aphthous ulceration. *N. Engl. J. Med.*, **355**, 165–172 (2006).
39) Khaled SA, Alexander MR, Wildman RD, Wallace MJ, Sharpe S, Yoo J, Roberts CJ. 3D extrusion printing of high drug loading immediate release paracetamol tablets. *Int. J. Pharm.*, **538**, 223–230 (2018).